Optical and Quantum Electronics (2024) 56:103
https://doi.org/10.1007/s11082-023-05654-3

Improving the physical and optical characteristics of Zinc doped borate glass for bone replacement

N. M. Salatein[1] · A. M. Abdelghany[2,3] · I. S. Fahim[1] · F. A. ElHussiny[4] · Y. Abdou[4]

Received: 4 October 2023 / Accepted: 25 October 2023 / Published online: 13 December 2023

Abstract
The presented study explores the potential of zinc-doped modified borate glass as a biomaterial for bone bonding applications. The glass samples were prepared using a melt quenching technique with a definite composition of (45-x) B_2O_3–24.5Na_2O–24.5CaO–6P_2O_5–xZnO, where $x = 1$, 2, 5, 7.5, and 10 (wt.%) and soaked in SBF for extended periods to explore their suitability for bone bonding applications. XRD and FTIR analysis were used to examine the structural properties of the samples before and after immersion in SBF. XRD analysis of the prepared samples reveals their amorphous nature before immersion. However, after four weeks of immersion, the XRD spectra show a reduction in the broad band observed at 2θ angles between 20 and 35°, indicating increased crystallization and the formation of a HA layer. FTIR data demonstrates significant modifications in the spectra after immersion, including the disappearance of certain bands and an increase in bands related to (BO_4) units. Additionally, the appearance of a new band at approximately 561 cm^{-1} confirms the formation of crystalline apatite. SEM images confirm the morphological changes, with a transition from a rough surface to a cotton shape, indicative of apatite formation. Electronic spectrum measurements (UV/Vis) were used to assess the samples' optical characteristics, showing that increasing Zn content decreases the optical energy gap, indicating improved optical properties. These findings highlight the structural, morphological, and optical changes induced by zinc ion doping and immersion in SBF, making it a more viable option for bone replacement.

Keywords Borate bioglass · Deconvolution analysis technique (DAT) · FTIR spectroscopy · ZnO

1 Introduction

Bioactive glasses based on silica have been broadly investigated in the application of bone replacement for the reason that they can form a bone-like mineral layer called hydroxy-carbonated apatite (HCA) on their surfaces as they are immersed in both in vivo and in vitro physiological fluid (Hench 2006a, 2006b; Hench 1998). Due to their lower chemical endurance, glasses based on borate have recently been exposed to a faster conversion to HCA than silicate-based glasses (Abdelghany et al. 2012; DE et al. 2003; Han and Day 2007;

Extended author information available on the last page of the article

Huang et al. 2006; Yao et al. 2007). It is commonly known that borate based on glasses has good thermal stability, a low melting point, and great transparency(Abdelghany and Rammah 2021; Kaky et al. 2019).Additionally, the creation of BO_3 triangular and BO_4 tetrahedral (non-bridged oxygen) units results in the formation of several structural units in borate glasses, including pentaborate, diborate, triborate, and tetraborate (Issa et al. 2019).

Wound healing and bone repair are the two primary study areas where borate bioactive glass are being investigated (Ege et al. 2022). Quicker conversion times may result in quicker healing, as has been shown in a variety of in vivo bone defect models; therefore, increased HCA conversion rates may be favourable for mineralized tissue repair (Bi et al. 2013; Fu et al. 2010; Wang et al. 2014). Glasses based on borate have also been effectively utilized as substrates for bone infection treatment given that they can be overloaded with antibacterial drugs, for instance, gentamicin (Cannio et al. 2021), vancomycin (Prasad et al. 2018), and teicoplanin (Ege et al. 2022; Homaeigohar et al. 2022; Zhang et al. 2010). Additionally, more recent research into the potential uses of glasses made of borate has included soft tissue applications like nerve restoration (Gupta et al. 2016; Krishnamacharyulu et al. 2018) and wound healing (Cannio et al. 2021; Liu et al. 2013; Rau et al. 2020; Zhao et al. 2015). A significant number of research investigations have been conducted on the development of bioactive glasses, and they have demonstrated that these glasses can be used to replace, regenerate, or repair injured body components. The outstanding qualities of the bioactive glass include its bioactivity, biocompatibility, and capacity to promote cell proliferation along with facilitating bone induction. The characteristics of the implant surface substantially influence these remarkable characteristics (Schuhladen et al. 2018). A conventional technique for producing bioactive glasses (BGs) is the melt-quench process, which entails melting precursor oxide powders at high temperatures and quickly chilling them to retain the amorphous network. This process is frequently used to create borate BGs, although it needs specific tools (Kermani et al. 2023).

Depending on the composition, diverse therapeutic active ions, for instance, B, Ca, Si, P, Ca, etc., have been released into the human system through the implantation of BGs. More research is being done on BGs with these biological ions, which provide a specific, dose-dependent response as antibacterial agents, angiogenesis enhancers, and osteogenesis motivation factors (Abouelnaga et al. 2021; Kargozar et al. 2018). Typically, modest amounts of these ions can be integrated into the glass structure as metallic ions like Cu^{+2}, Ag^{+2}, Mg^{+2}, Zn^{+2}, Fe^{+3}, Sr^{+2}, and Co^{+2} (Ghazy et al. 2023b; Ram and Ram 1996, 1988). Numerous alkali metals, including ZnO, Na_2O, CaO, and MgO, work as excellent modifiers in glasses that enhance their optical and structural characteristics(Abouhaswa et al. 2020).Zinc oxide (ZnO) is a commonly used substance in both medicinal and industrial uses(Rashad et al. 2020). Zinc (Zn) is an essential element during bone metabolism since it is a cofactor for several enzymes. Zn is used in the structure of several metalloenzymes because of its ability to induce bone formation (Thanasrisuebwong et al. 2022) by stimulating the synthesis of protein, which is required for DNA replication in osteoblast cells, increasing alkaline phosphatase (ALP) activity in bone, preventing bone resorption(Yamaguchi 2010), increasing bone mass (Ghazy et al. 2023a) and preventing bacterial infections (Heras et al. 2020; Lang et al. 2007; Schuhladen et al. 2020).In addition, Zn is a critical component for wound healing in soft tissue regeneration (Hench 2006a, 2006b; Saranti et al. 2006). Investigations have also demonstrated that small quantities of Zn induced early cell proliferation and enhanced differentiation of in vitro biocompatibility studies. Furthermore, research has shown that tiny amounts of Zn improved differentiation and stimulated early cell proliferation in vitro biocompatibility investigations (Balamurugan et al. 2007; Lakhkar et al. 2013; Oki et al. 2004).The significant calcification alterations that are caused by deficiencies in

zinc are associated with a reduction in bone density and slower skeletal growth (Li et al. 2022; Yamaguchi 2010). In the glass structure, ZnO may function as a network modifier, an intermediate oxide, or both. It was revealed that ZnO acts as a network modifier up to a certain concentration, but that when the ZnO content grew, it became an intermediate oxide (Afrizal et al. 2020; El-Kady and Ali 2012; Subhashini et al. 2014). Zinc can eliminate cations from the network of silica, forming a new bond (Si–O–Zn) with significantly lower strength than the Si–O–Si link and therefore lowering the glass transition temperature.In the SBF solution, Zn helped maintain the pH within the physiological range by generating zinc hydroxide. In vitro biocompatibility tests have confirmed that zinc in small quantities enhances the earliest stages of cell division and proliferation (Oki et al. 2004), but adding zinc can delay the bioactive glasses' degradation profile (Haimi et al. 2009). Furthermore, the addition of ZnO to the borate glass system improves its glass-forming ability, reduces the melting temperature, and decreases the rate of crystallization.

Several ZnO–containing borate glasses have shown promising outcomes in vitro investigations (Abdelghany et al. 2014). Thus, after immersion in SBF solution, the synthesis of hydroxyapatite is enhanced by increasing the concentration of Zn ions in the composition of borate glass.Numerous investigations have revealed that BBGs may help to rebuild bone in vivo without causing cytotoxicity (Thyparambil et al. 2020) (Sengupta et al. 2021).

In this investigation, the novelty of the present work is to report structural, physical, and optical investigations on new zinc-doped borate glasses to obtain the optimum glass system for targeted bone replacement application.

2 Materials and methods

2.1 Sample preparation

Zinc-doped, modified borate Hench bioglasses of the compositional (45–x) B_2O_3–24.5Na_2O–24.5CaO–6P_2O_5–xZnO, where $x = 1$, 2, 5, 7.5, and 10 (wt.%); were produced by the traditional melt quenching process. In Table 1, B_2O_3 was gradually replaced with zinc oxide (ZnO) to investigate the role of the addition of Zn on the glassy structure.

Briefly, B_2O_3 that is obtained from an orthoboric acid source (Sigma-Aldrich Co.) was initially mixed with the other weighted batches of P_2O_5 obtained from an ammonium dihydrogen phosphate source and supplied by Sigma-Aldrich Co., calcium, and sodium carbonates (El-Nasr Pharmaceuticals), with gradually added ZnO replacing the borate partner. After that, the mixture was placed into an agate mortar and heated to a temperature of around 1050 °C (± 10 °C) in crucibles that were crusted with platinum. At intervals of 30 min, the crucibles were rotated to obtain adequate homogeneity following the glass' composition. To form the

Table 1 Sample composition of the modified borate bioglass wt.%

Glass sample	B2O3	CaO	Na2O	P2O5	ZnO
Zn1	44	24.5	24.5	6	1
Zn2	43	24.5	24.5	6	2
Zn5	40	24.5	24.5	6	5
Zn7.5	37.5	24.5	24.5	6	7.5
Zn10	35	24.5	24.5	6	10

glass, the molten mixture was then quenched and pressed between two steel plates at room temperature. The same preparation technique that Kokubo et al. previously disclosed was used to create an SBF solution with ion concentration about equivalent to that of human blood plasma (Kokubo and Takadama 2006).

2.2 Characterization techniques

XRD, FTIR, SEM, and EDAX studies were carried out to characterize the compositional and structural changes within the glasses caused by the reaction that occurred with the SBF solution. The crystalline phases that were present or created inside the sample before and post-soaking for up to four weeks in the SBF solution at 37 °C will be identified by examining the BG sample phase constituents using the X-ray diffraction (XRD) technique.

Brucker Axs-D8 setup and a copper radiation source K-line at 0.154600 nm over a 2 range of 4 to 70 with a step size of 0.02, XRD spectral data were produced. With a period of 0.4 s and an interval of 0.020, data was steeply collected. Utilizing the Joint Committee on Powder Diffraction and Standards, the resulting spectra were compared to the compiled standards (JCDPS).Using Fourier Transformation Infrared Spectroscopy (FTIR), compositional alterations coupled with structural modifications in qualitative or quantitative ways were discovered. A single-beam Fourier transform infrared spectrometer (Nicolet IS10, ThermoFisher Co.) was used to get the FTIR absorption spectra for several substances at room temperature. To analyze the samples' structures, with a resolution of 2.0 cm^{-1}, absorbance-mode FTIR spectra were scanned over a wavenumber range of 400–400 cm^{-1}. The glass pieces were crushed to powder and combined with KBr at a weight proportion of 1:100 for the IR examination in absorption mode. To avoid a moisture attack, IR absorption spectra were taken right away. Each glass sample's spectrum is an average of individual scans that have been standardized to the spectrum. Background and dark current noises were removed from the spectra obtained. It was carried out at Mansoura University's Fine Measurements Laboratory, which is part of the faculty of science. The obtained FTIR spectra were quantitatively evaluated and stimulated by Gaussian functions using a standard curve fitting tool (peak fit 4.12) that modified the peak positions of each band's intensities and widths in two steps as previously indicated(Abdelghany et al. 2023). The relative area of both (BO_3) and (BO_4) units in the following peaks, which were analyzed using the formula below, was used to quantify the amount of borate glass N4:

$$N4 = \frac{\mathbf{BO}4}{\mathbf{BO}4 + \mathbf{BO}3}$$

Using a scanning electron microscope (SEM) with a JEOL JSM-6510LV, USA, operating at a 20 kV accelerating voltage, the morphology of the films was examined. To shrink the charging effects of the sample from the electron beam, a thin layer of gold (3.5 nm) was applied to the samples' surfaces using the vacuum evaporation process. To examine how the addition of the dopant altered the structures of the samples and their optical properties, UV/Vis absorption spectra were obtained using a spectrophotometer (JASCO 630, Japan).

3 Results and discussion

3.1 X-ray diffraction analysis

Figure 1 shows the XRD diffraction pattern of the prepared powder of borate glasses samples with nominal composition (B_2O_3) ($45B_2O_3$, 24.5CaO, $24.5Na_2O$, $6P_2O_5$) doped with different concentrations of zinc ions (Zn) (1, 2, 5, 7.5, and 10%) prior and after soaking in SBF between 5 and 70 °C Bragg angle range at room temperature. Sample notations and compositions are listed in the table above. Before immersion, the diffraction patterns of all prepared samples reflect their amorphous nature without any evidence for crystallization or phase separation, despite the rising content of Zn ions to 10 wt.%, as recognized from glass definition by various glass researchers (Mardas et al. 2021). After spending four weeks submerged in SBF, XRD data illustrate that the broad band of all samples that appears in XRD spectra in Fig. 1 at 2 theta angles approximately between (20–35°) is diminished after 4 weeks of immersion, and glass appears to be more crystallized, with little diffraction peak that relates to crystalline phases related to the formation of a hydroxyapatite layer (Huang et al. 2006).

3.2 SEM and EDX analysis

In SEM Fig. 2 of the MBHG doped with 5 and 10 wt.% of Zn doped borate glass before immersion in SBF solution indicates the amorphous borate matrix as a roughed sample is the continuous phase and is present as a dominant structure. This would be reflected from the energy dispersive X-ray (EDX) spectrum of 10 wt% of Zn doped MBHGs as in Fig. 3 in which B and Ca atoms are considered the most dominant constituents in the tested sample.

Figure 4 presents SEM images of the samples containing 5 wt.% and 10 wt.% of Zinc-doped borate glass After 4 weeks of immersion in SBF solution. These figures showed

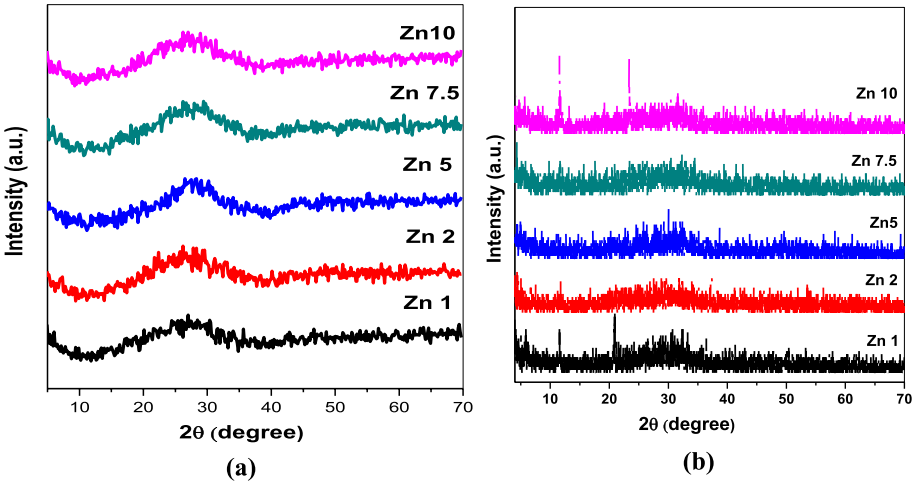

Fig. 1 XRD spectrum of glass samples doped with Zn **a** before soaking in SBF **b** after soaking in SBF

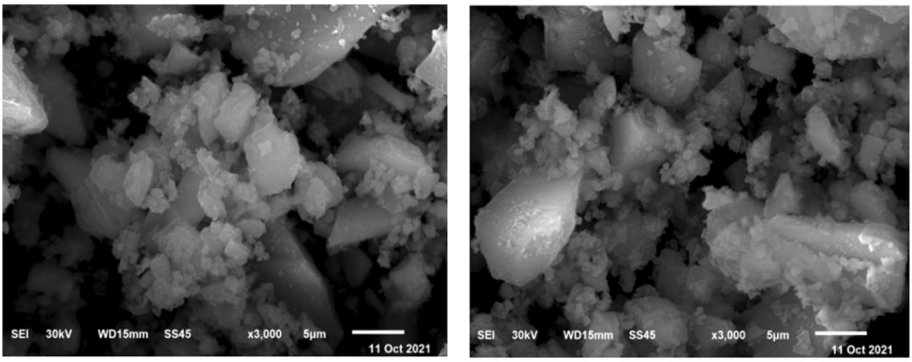

Fig. 2 SEM for glass doped with Zn before soaked in SBF solution in case of **a** 5 wt%, **b** 10wt%

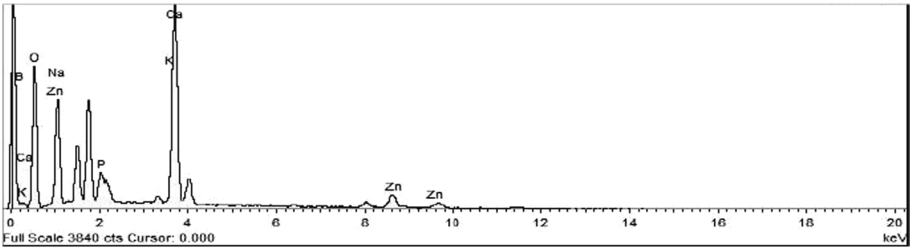

Fig. 3 EDAX for glass doped with 10wt% of Zn before soaked in SBF solution

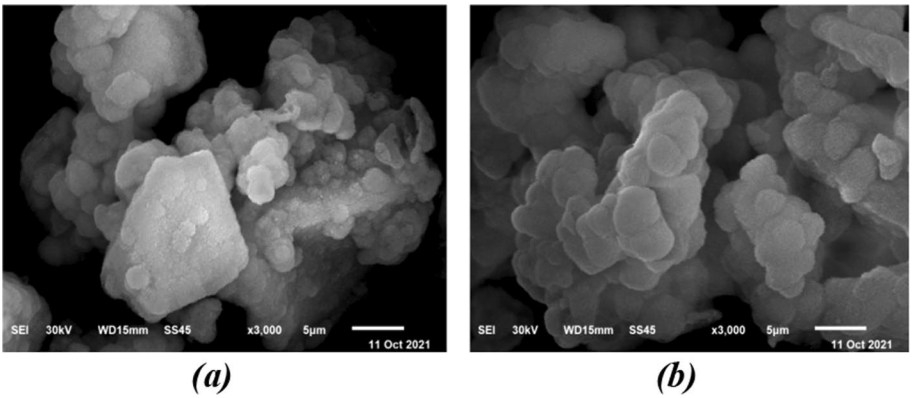

Fig. 4 SEM for glass doped with Zn after soaked in SBF solution in case of **a** 5 wt.%, **b** 10wt%

significant changes to the surface morphology; from a roughed surface to a surface with a cotton shape, evidencing the morphology of the apatite formed.

Figure 5 shows the EDX spectrum obtained due to a reaction time of 4 weeks between the sample (10 wt.%) of Zn-doped MBHGs and SBF. From the results, it appeared that

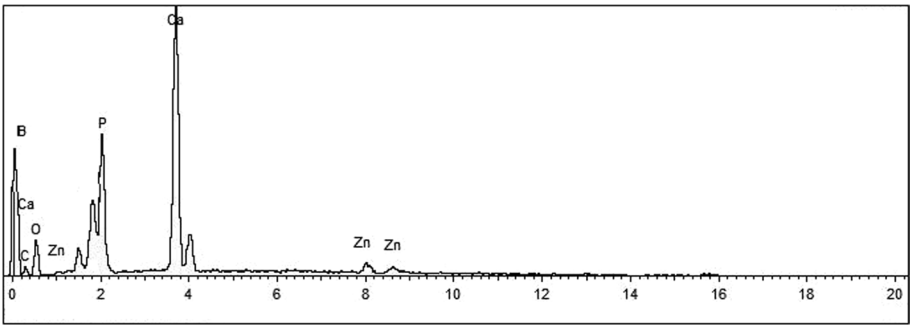

Fig. 5 EDAX for glass doped with 10wt% of Zn after soaked4 weeks in SBF solution

when bioglass is soaked in SBF for a lengthy period (4 weeks), the hydroxyapatite layer forms and precipitates on top of the surfaces and spreads over the entire surface. Our considerations based on SEM observations indicate that increasing Zn concentration affects HA layer formation and agrees well with previously XRD-reported results.

3.3 Fourier transform infrared (FTIR)

The absorption spectra chart of FTIR of Zn-doped materials with dissimilar concentrations before soaking in the solution of SBF is shown in Fig. 6. The presence of dopant Zn ions led to the emergence of a broad, tiny band at 1218 cm^{-1}, which was recognized as the formation of non-bridging oxygen (NBO) associated with increasing in trigonal units (BO_3), and this band intensity enlarged as the Zn concentration increased.

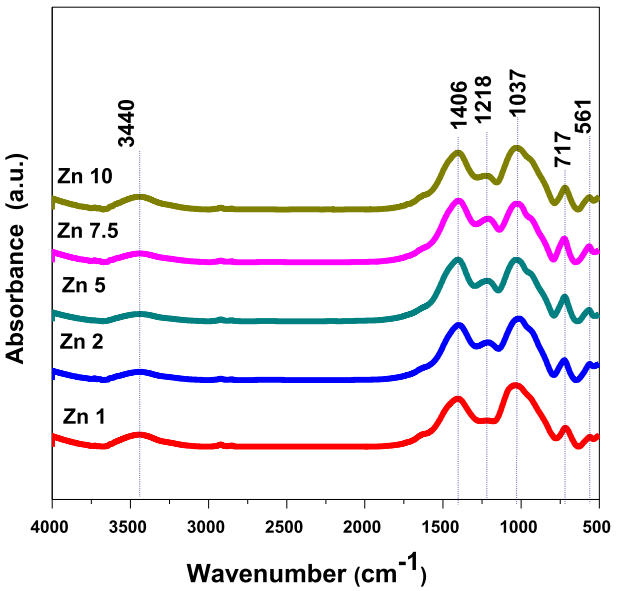

Fig. 6 FTIR spectra of Zn doped borate glass sample before immersion in SBF

As shown in Fig. 7 we studied the effect of concentration on prepared samples of glass that have been soaked in SBF for a total period of 1, 2, 3, and 4 weeks. FTIR spectrum observations of the Zn system indicate that the bands at 3433 cm^{-1} correspond to the modes of stretching vibration correspondingly of the hydroxyl group (Asthana and Heise 2011) and communicate to H_2O adsorption at the surface. 1409 cm^{-1} peak is assigned to the bending C–O vibration of carboxyl groups ($CO3^{-2}$) found in the HCA structure (Pino et al. 2008).The strong bands at 1035 cm^{-1} match up to vibration modes for P-O that are related to the amorphous calcium phosphate layer, and they increase in intensity with immersion time (3 and 4 weeks), whereas the peaks at 719 and 562 cm^{-1} correspond to O–P–O bending modes (Elzinga and Sparks 2007). The phosphate mode appears as a resolved small single peak at 463 cm^{-1} in the case of 1 wt.% Zn and is assigned to the asymmetric mode of P-O vibrations in amorphous calcium phosphate (apatite). The IR spectra of the examined borate glasses exhibit this significant modification in the spectra after immersion:

1. The disappearance of the bands at 718 cm^{-1} from the first week in the case of Zn concentration (1, 5, and 10) disappeared from 2 weeks for 7.5 wt.% of Zn and just from 4weeks for 2 wt.% of Zn and this confirms the ion exchange process of glass.
2. The disappearance of the bands at 1218 $cm^{-1}$for all concentrations from the first week that related to triangular units (BO_3) confirms increasing the bands related to (BO_4).

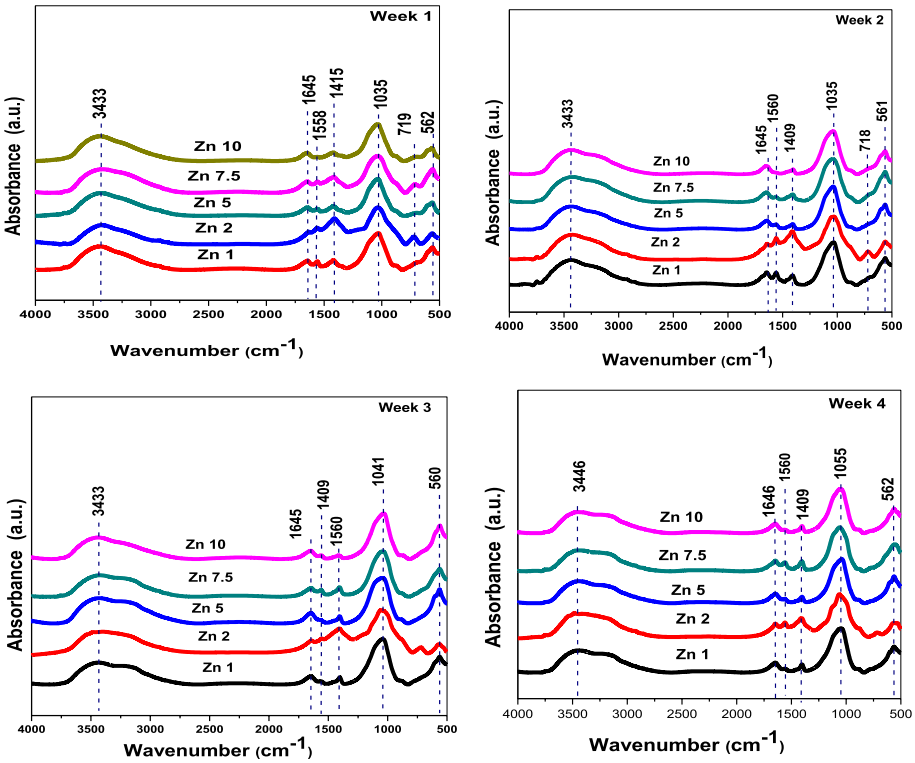

Fig. 7 Zn sample FTIR spectra after soaking for **a** 1 week, **b** 2 weeks, **c** 3 weeks, and **d** 4 weeks

3. The substantial persistence of the major band at roughly 1035 cm^{-1} following corrosion with SBF solution, as well as the quiet fall in the intensities of the band 1560 cm^{-1}, show that the bands related to BO_3 vibrations are greatly reduced, but the bands due to BO_4 vibrations endure and remain noticeable.
4. The new band peaks at about 561 cm^{-1}confirm the formation of crystalline apatite, which was documented by SEM morphology and XRD results.

Comparing the FTIR absorption spectra of glasses with different amounts of ZnO in Fig. 7, it is deduced that the sample containing a higher concentration of ZnO possesses not only higher crystallinity but also more phases than that in the glass containing a lower one. This observation is highly confirmed by the results based upon EDX analysis of Ca and P content in crystalline phases (Fig. 5), XRD patterns (Fig. 1b), and SEM morphology (Fig. 4) of the obtained bioactive apatite phases.

Figure 8 shows a deconvolution analysis of samples comprising zinc oxide amounts of 10 wt.%, which were utilized to evaluate the four-coordinated boron (N4) changes before and after 1, 2, 3, and 4 weeks of soaking in SBF solution. As previously reported by several authors, the deconvolution technique is based on prior knowledge of the wave number of proposed vibrational groups and the second derivative of the spectrum, which specifies the precise position of peak maxima(Abdelghany et al. 2022; Abdelghany 2010; Lin et al. 2022).

The N4 fraction for ZnO doped borate glasses of the concentration of (1, 10 wt.%) was tabulated as shown in Table 2 and it is represented in Fig. 9 for different immersion times (1, 2, 3, and 4) to estimate indicates boron atoms transformations occur during immersion time in SBF solution. The value of N4 is thought to have increased with longer immersion times before beginning to decline in the last week. In addition to other parameters, the development of NBO can be linked to a reduction in the ratio of N4 when immersion time is increased. Higher-wavelength electron excitation is facilitated by the negative charge on NBOs (Chanshetti et al. 2011). By increasing the quantity of NBO atoms, ZnO improved the glass network and decreased the $BO_4/(BO_4+BO_3)$ ratio (Boda et al. 2016). ZnO operates as an intermediate oxide in the glass structure, either as a modifier or a maker network (Ahmad et al. 2014).

3.4 UV–vis. spectroscopic measurements

Using ultraviolet–visible absorption spectroscopy, the optical characteristics of a material that reveal information about its electronic structure can be represented(kenawy et al. 2022; Taha and Rammah 2016). The wavelength range of UV/Vis absorption spectra is between 200 and 1100 nm as shown in Fig. 10. The samples display two absorption peaks at approximately 243 and 238 nm in the spectrum UV region for all glass samples doped with Zn, which result from the iron impurities that are an obligatory tracer inside the raw materials during the glass formation (ElBatal et al. 2009). The absorbance is approximately the same in the concentration (1 and 7.5) wt.% of Zn, and concentration 2 wt.% is the least one in absorbance. Internal and external factors such as electronic transitions, chemical bonding, and the glass structure, which are primarily caused by the addition of dopants, influence the UV absorption of glasses (Elbatal et al. 2011).Also, the absorption edge position change is caused by the oxygen bondingvariation within the glass network (El Agammy et al. 2021).The metal cations addition for example Pb, Zn, Cd, etc., affects the B_2O_3 and SiO_4 network formation. These cation additives can also act as a nucleating

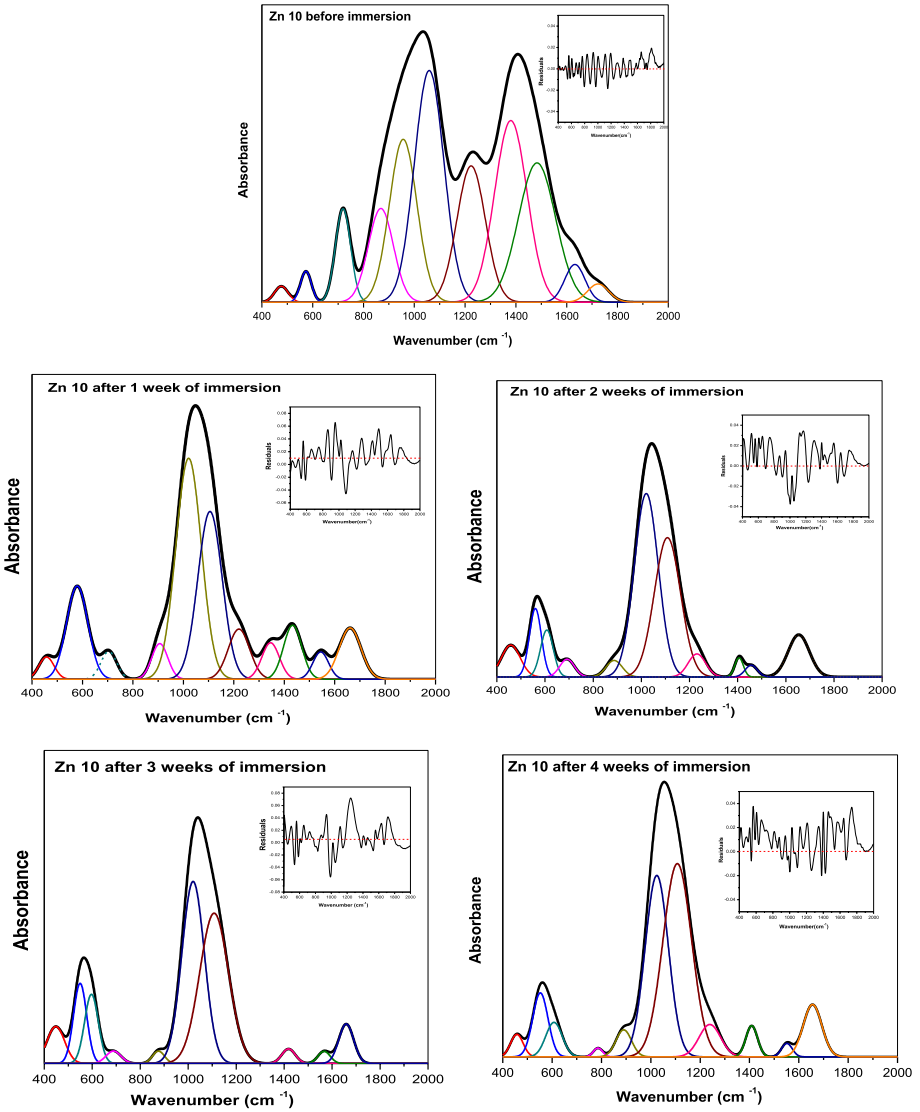

Fig. 8 Deconvolution and residual results of Zinc doped 45S5 borate bioactive with the addition of 10 wt.% of ZnO before and after soaking in SBF solution

Table 2 The N4 fraction calculated before and post-soaking in the solution of SBF

Zn conc	N4				
	Before	1 Week	2 Weeks	3 Weeks	4 Weeks
1	0.521	0.748	0.842	0.880	0.785
10	0.455	0.743	0.808	0.941	0.846

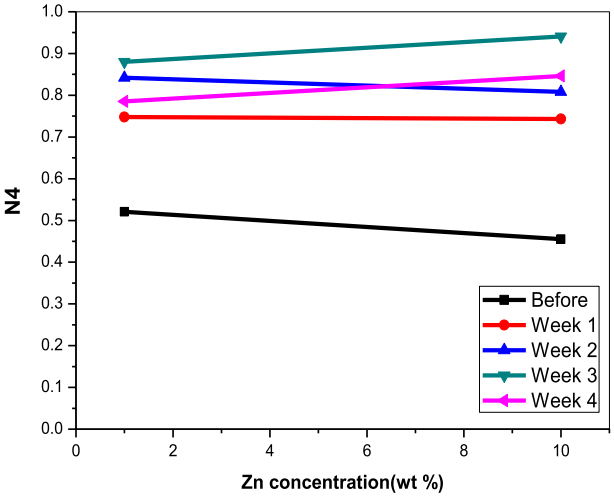

Fig. 9 Illustrate N4 variation as a function of the concentration of zinc oxide and soaking time

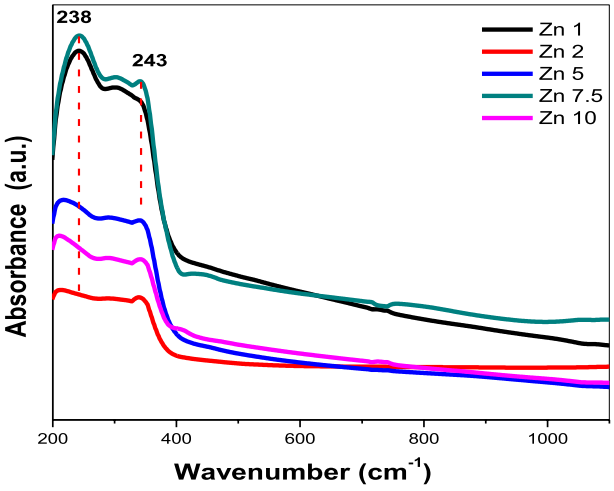

Fig. 10 Spectra of UV/Vis for Borate glass containing Zn by 1, 2, 5, 7.5, and 10 wt.%

agent for glass crystallization and a network modifier. Therefore, the borate glasses' optical properties have significantly changed (Gautam et al. 2012).

The optical energy gap (Eg) values are recorded in Table 3 and shown in Fig. 11. The values of indirect and direct band gap were reduced with an increase in the dopant concentrations.

4 Conclusions

In this paper glass of supposed composition [(45-*x*) B_2O_3–24.5Ca O–24.5Na_2O–6P_2O_5–*x* ZnOWt.%], while x = 1, 2, 5, 7.5, and 10 Wt.% were successfully been prepared through a melt quenching route. In conclusion, the experimental results obtained from the XRD, SEM, EDX, and FTIR analyses provide valuable insights into the structural and morphological changes that occur in borate glasses doped with different concentrations of zinc

Table 3 The effect of varying Zinc oxide concentrations on the optical characteristics of borate glass

Sample	Absorption edge (λg) (nm)	E optical (eV)	Edirect (eV)	E indirect(eV)
Zn 1	455.03	2.73	2.22	3.09
Zn2	438.72	2.83	2.32	3.16
Zn5	432.42	2.87	2.31	3.18
Zn7.5	429.08	2.89	2.37	3.21
Zn10	419.44	2.96	2.07	3.16

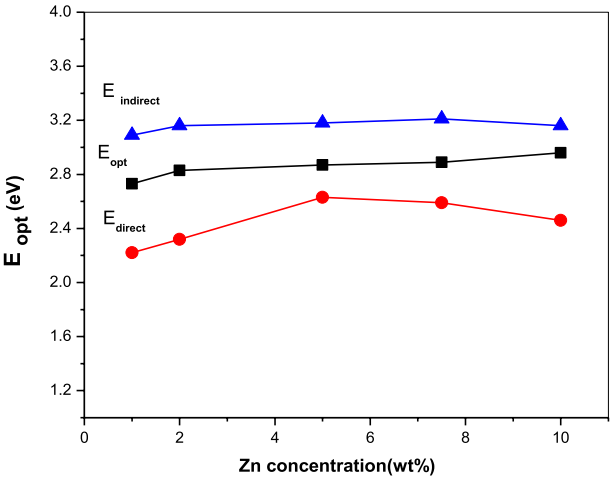

Fig. 11 Indirect and direct band gap energies as a function of Zinc concentration in the glassy matrix

ions before and after immersion in simulated body fluid (SBF). The XRD analysis of the samples before immersion revealed their amorphous nature, with no evidence of crystallization or phase separation, even with the increasing concentration of zinc ions. However, after four weeks of immersion, the XRD data showed a reduction in the broad band observed in the diffraction pattern, indicating increased crystallization and the formation of a hydroxyapatite layer.

SEM images of the samples before immersion displayed an amorphous borate matrix as the dominant structure, with rough surface morphology. However, after immersion, significant changes in surface morphology were observed, with the formation of a cotton-shaped hydroxyapatite layer. The EDX analysis confirmed that boron and calcium were the dominant constituents in the tested samples, especially in the case of 10 wt.% zinc-doped borate glass immersed in SBF for four weeks. FTIR analysis revealed several modifications in the spectra after immersion. The disappearance of certain bands indicated an ion exchange process between the glass and SBF solution. The emergence of new peaks confirmed the formation of crystalline apatite. The intensity of certain bands related to BO_3 vibrations decreased, while those related to BO_4 vibrations remained visible. The UV/Vis absorption spectra showed two absorption peaks resulting from iron impurities in the raw materials used for glass formation. The addition of zinc ions influenced the optical properties of the borate glasses, and the absorbance varied with different zinc concentrations. Overall, the experimental findings suggest that the addition of zinc ions to borate glasses affects their

structural, morphological, and optical properties. The immersion in SBF leads to the formation of a hydroxyapatite layer on the glass surface, and the concentration of zinc ions influences the crystallization and morphology of the formed layer.

The study investigates the impact of zinc oxide on the physical properties, bioactivity of borate-based bioactive glass for bone bonding application.

Acknowledgements This paper is based on work supported by the Science Technology & Innovation Funding Authority (STDF) under a grant (45610).

Author contributions NMS: Conceptualization, Methodology, Formal analysis, Investigation, Writing—Original Draft—Review & Editing; AMA: Supervision, Conceptualization, Methodology, Formal analysis, Investigation, Writing—Original Draft , reviewing Final version; ISF: Conceptualization, Methodology, Writing—Review & Editing; FAE: Conceptualization, Methodology, Formal analysis, Investigation, Writing—Review & Editing; YA: Supervision, Conceptualization, Methodology, Writing—Review & Editing.

Funding Open access funding provided by The Science, Technology & Innovation Funding Authority (STDF) in cooperation with The Egyptian Knowledge Bank (EKB). The Science Technology & Innovation Funding Authority (STDF) (45610, 45610, 45610, 45610, 45610).

Declarations

Competing interests The authors declare no competing interests.

References

Abdelghany, A.M.: The elusory role of low level doping transition metals in lead silicate glasses. Silicon **2**, 179–184 (2010). https://doi.org/10.1007/s12633-010-9053-8

Abdelghany, A.M., Rammah, Y.S.: Transparent alumino lithium borate glass-ceramics: synthesis, structure and gamma-ray shielding attitude. J. Inorg. Organomet. Polym. Mater. **31**, 2560–2568 (2021). https://doi.org/10.1007/s10904-020-01862-6

Abdelghany, A.M., Elbatal, H.A., Ezzeldin, F.M.: Bone bonding ability behavior of some ternary borate glasses by immersion in sodium phosphate solution. Ceram. Int. **38**, 1105–1113 (2012). https://doi.org/10.1016/j.ceramint.2011.08.038

Abdelghany, A.M., ElBatal, F.H., ElBatal, H.A.: Zinc containing borate glasses and glass-ceramics: search for biomedical applications. Process. Appl. Ceram. **8**, 185–193 (2014). https://doi.org/10.2298/PAC1404185A

Abdelghany, A.M., Diab, H.M., Madbouly, A.M., Ezz-ElDin, F.M.: Inspection of Radiation shielding proficiency and effect of gamma-ray on ESR and thermal characteristics of copper oxide modified borate bioglasses. J. Inorg. Organomet. Polym. Mater. **32**, 3204–3219 (2022). https://doi.org/10.1007/s10904-022-02349-2

Abdelghany, A.M., Mahmoud, N., Abdou, Y., El-Husseiny, F.: Novel strontium borate modified hench`s bioglass synthesis and characterization for bone replacement. Biointerface Res. Appl. Chem. **13**, 1–10 (2023). https://doi.org/10.33263/BRIAC131.019

Abouelnaga, A.M., Meaz, T.M., Othman, A.M., Ghazy, R.A., El Nahrawy, A.M.: Probing the structural and antimicrobial study on a sol-gel derived velosef-loaded bioactive calcium magneso-silicate xerogel. Silicon **13**, 623–631 (2021). https://doi.org/10.1007/s12633-020-00448-8

Abouhaswa, A.S., Al-Buriahi, M.S., Chalermpon, M., Rammah, Y.S.: Influence of ZrO_2 on gamma shielding properties of lead borate glasses. Appl. Phys. A Mater. Sci. Process. **126**, 1–11 (2020). https://doi.org/10.1007/s00339-019-3264-7

Afrizal, N.H., Yahya, N., Yusoff, N.M., Kasim, A., Hashim, A.: Physical, mechanical and structural properties of yttrium oxide doped zinc borate glasses. Solid State Phenom. **307**, 327–335 (2020). https://doi.org/10.4028/www.scientific.net/SSP.307.327

Ahmad, F., Hassan Aly, E., Atef, M., Elokr, M.M.: Study the influence of zinc oxide addition on cobalt doped alkaline earth borate glasses. J. Alloys Compd. **593**, 250–255 (2014). https://doi.org/10.1016/j.jallcom.2014.01.067

Asthana, B.P., Heise, H.M.: Vibrational Spectroscopy. Elsevier, Amsterdam (2011)

Balamurugan, A., Balossier, G., Kannan, S., Michel, J., Rebelo, A.H.S., Ferreira, J.M.F.: Development and in vitro characterization of sol-gel derived $CaO–P_2O_5$-SiO_2-ZnO bioglass. Acta Biomater. **3**, 255–262 (2007). https://doi.org/10.1016/j.actbio.2006.09.005

Bi, L., Rahaman, M.N., Day, D.E., Brown, Z., Samujh, C., Liu, X., Mohammadkhah, A., Dusevich, V., Eick, J.D., Bonewald, L.F.: Effect of bioactive borate glass microstructure on bone regeneration, angiogenesis, and hydroxyapatite conversion in a rat calvarial defect model. Acta Biomater. **9**, 8015–8026 (2013). https://doi.org/10.1016/j.actbio.2013.04.043

Boda, R., Srinivas, G., Komaraiah, D., Shareefuddin, M., Sayanna, R.: Optical properties of bismuth borate glasses doped with Eu^{3+} ions. AIP Conf. Proc. **1728**, 020377 (2016). https://doi.org/10.1063/1.4946428

Cannio, M., Bellucci, D., Roether, J.A., Boccaccini, D.N., Cannillo, V.: Bioactive glass applications: a literature review of human clinical trials. Materials (Basel). **14**, 1–25 (2021). https://doi.org/10.3390/ma14185440

Chanshetti, U.B., Sudarsan, V., Jogad, M.S., Chondhekar, T.K.: Effect of CuO addition on the optical and electrical properties of sodium zinc borophosphate glasses. Phys. B Condens. Matter. **406**, 2904–2907 (2011). https://doi.org/10.1016/j.physb.2011.04.063

De, D., Je, W., Rf, B., Kd, M.: Transformation of borate glasses into biologically useful materials. Glas. Technol. **44**, 75–81 (2003)

Ege, D., Zheng, K., Boccaccini, A.R.: Borate bioactive glasses (BBG): bone regeneration, wound healing applications, and future directions. ACS Appl. Bio Mater. **5**, 3608–3622 (2022). https://doi.org/10.1021/acsabm.2c00384

El Agammy, E.F., Doweidar, H., El-Egili, K., Ramadan, R.M.: Physical and optical properties of NaF–TeO_2 glasses and glass–ceramics. Appl. Phys. A Mater. Sci. Process. **127**, 1–9 (2021). https://doi.org/10.1007/s00339-020-04153-6

ElBatal, F.H., Hamdy, Y.M., Marzouk, S.Y.: UV-visible and infrared absorption spectra of transition metals-doped lead phosphate glasses and the effect of gamma irradiation. J. Non Cryst. Solids **355**, 2439–2447 (2009). https://doi.org/10.1016/j.jnoncrysol.2009.08.044

Elbatal, F.H., Marzouk, M.A., Abdelghany, A.M.: UV-visible and infrared absorption spectra of gamma irradiated V_2O_5-doped in sodium phosphate, lead phosphate, zinc phosphate glasses: a comparative study. J. Non Cryst. Solids **357**, 1027–1036 (2011). https://doi.org/10.1016/j.jnoncrysol.2010.11.040

El-Kady, A.M., Ali, A.F.: Fabrication and characterization of ZnO modified bioactive glass nanoparticles. Ceram. Int. **38**, 1195–1204 (2012). https://doi.org/10.1016/j.ceramint.2011.07.069

Elzinga, E.J., Sparks, D.L.: Phosphate adsorption onto hematite: an in situ ATR-FTIR investigation of the effects of pH and loading level on the mode of phosphate surface complexation. J. Colloid Interface Sci. **308**, 53–70 (2007). https://doi.org/10.1016/j.jcis.2006.12.061

Fu, Q., Rahaman, M.N., Fu, H., Liu, X.: Silicate, borosilicate, and borate bioactive glass scaffolds with controllable degradation rate for bone tissue engineering applications. I. Preparation and in vitro degradation. J. Biomed. Mater. Res. Part A **95**, 164–171 (2010). https://doi.org/10.1002/jbm.a.32824

Gautam, S.P., Bundela, P.S., Pandey, A.K., Jamaluddin, Awasthi, M.K., Sarsaiya, S.: Diversity of cellulolytic microbes and the biodegradation of municipal solid waste by a potential strain. Int. J. Microbiol. **2012**, 325907 (2012). https://doi.org/10.1155/2012/325907

Ghazy, A., Al-Hossainy, A., El-Sheekh, M., Makhlof, M.: Investigating the differences in structure, morphology, optical properties, laser photoluminescence and dielectric properties for chitosan-doped commercial and Polycladia myrica mediated ZnO nanoparticles films combined with TD-DFT simulations. Algal Res. **71**, 103076 (2023). https://doi.org/10.1016/j.algal.2023.103076

Ghazy, A.R., Elmowafy, B.M., Abdelghany, A.M., Meaz, T.M., Ghazy, R., Ramadan, R.M.: Structural, optical, and cytotoxicity studies of laser irradiated ZnO doped borate bioactive glasses. Sci. Rep. **13**, 1–12 (2023). https://doi.org/10.1038/s41598-023-34458-4

Gupta, B., Papke, J.B., Mohammadkhah, A., Day, D.E., Harkins, A.B.: Effects of chemically doped bioactive borate glass on neuron regrowth and regeneration. Ann. Biomed. Eng. **44**, 3468–3477 (2016). https://doi.org/10.1007/s10439-016-1689-0

Haimi, S., Gorianc, G., Moimas, L., Lindroos, B., Huhtala, H., Räty, S., Kuokkanen, H., Sándor, G.K., Schmid, C., Miettinen, S., Suuronen, R.: Characterization of zinc-releasing three-dimensional bioactive glass scaffolds and their effect on human adipose stem cell proliferation and osteogenic differentiation. Acta Biomater. **5**, 3122–3131 (2009). https://doi.org/10.1016/j.actbio.2009.04.006

Han, X., Day, D.E.: Reaction of sodium calcium borate glasses to form hydroxyapatite. J. Mater. Sci. Mater. Med. **18**, 1837–1847 (2007). https://doi.org/10.1007/s10856-007-3053-2

Hench, L.L.: Biomaterials: a forecast for the future. Biomaterials **19**, 1419–1423 (1998). https://doi.org/10.1016/S0142-9612(98)00133-1

Hench, L.L.: The story of Bioglass®. J. Mater. Sci. Mater. Med. **17**, 967–978 (2006a). https://doi.org/10.1007/s10856-006-0432-z

Heras, C., Jiménez-Holguín, J., Doadrio, A.L., Vallet-Regí, M., Sánchez-Salcedo, S., Salinas, A.J.: Multifunctional antibiotic- and zinc-containing mesoporous bioactive glass scaffolds to fight bone infection. Acta Biomater. **114**, 395–406 (2020). https://doi.org/10.1016/j.actbio.2020.07.044

Homaeigohar, S., Li, M., Boccaccini, A.R.: Bioactive glass-based fibrous wound dressings. Burn. Trauma. **10**, 038 (2022). https://doi.org/10.1093/burnst/tkac038

Huang, W., Day, D.E., Kittiratanapiboon, K., Rahaman, M.N.: Kinetics and mechanisms of the conversion of silicate (45S5), borate, and borosilicate glasses to hydroxyapatite in dilute phosphate solutions. J. Mater. Sci. Mater. Med. **17**, 583–596 (2006). https://doi.org/10.1007/s10856-006-9220-z

Issa, S.A.M., Susoy, G., Ali, A.M., Tekin, H.O., Saddeek, Y.B., Al-Hajry, A., Algarni, H., Anjana, P.S., Agar, O.: The effective role of La_2O_3 contribution on zinc borate glasses: radiation shielding and mechanical properties. Appl. Phys. A Mater. Sci. Process. **125**, 1–19 (2019). https://doi.org/10.1007/s00339-019-3169-5

Kaky, K.M., Sayyed, M.I., Laariedh, F., Abdalsalam, A.H., Tekin, H.O., Baki, S.O.: Stuctural, optical and radiation shielding properties of zinc boro-tellurite alumina glasses. Appl. Phys. A Mater. Sci. Process. **125**, 1–12 (2019). https://doi.org/10.1007/s00339-018-2329-3

Kargozar, S., Baino, F., Hamzehlou, S., Hill, R.G., Mozafari, M.: Bioactive glasses: sprouting angiogenesis in tissue engineering. Trends Biotechnol. **36**, 430–444 (2018). https://doi.org/10.1016/j.tibtech.2017.12.003

Kenawy, E.-R., Ghazy, A.R., Al-Hossainy, A.F., Rizk, H.F., Shendy, S.: Synthesis, characterization, TD-DFT method, and optical properties of novel nanofiber conjugated polymer. Synth. Met. **291**, 117206 (2022). https://doi.org/10.1016/j.synthmet.2022.117206

Kermani, F., Nazarnezhad, S., Mollaei, Z., Mollazadeh, S., Ebrahimzadeh-Bideskan, A., Askari, V.R., Oskuee, R.K., Moradi, A., Hosseini, S.A., Azari, Z., Baino, F., Kargozar, S.: Zinc- and copper-doped mesoporous borate bioactive glasses: promising additives for potential use in skin wound healing applications. Int. J. Mol. Sci. **24**, 1304 (2023). https://doi.org/10.3390/ijms24021304

Kokubo, T., Takadama, H.: How useful is SBF in predicting in vivo bone bioactivity? Biomaterials **27**, 2907–2915 (2006). https://doi.org/10.1016/j.biomaterials.2006.01.017

Krishnamacharyulu, N., Jagan Mohini, G., Sahaya Baskaran, G., Ravi Kumar, V., Veeraiah, N.: Investigation on Silver Doped B_2O_3–SiO_2–P_2O_5–Na_2O–CaO Bioglass System for Biomedical Applications. Elsevier, Amsterdam (2018)

Lakhkar, N.J., Lee, I.H., Kim, H.W., Salih, V., Wall, I.B., Knowles, J.C.: Bone formation controlled by biologically relevant inorganic ions: role and controlled delivery from phosphate-based glasses. Adv. Drug Deliv. Rev. **65**, 405–420 (2013). https://doi.org/10.1016/j.addr.2012.05.015

Lang, C., Murgia, C., Leong, M., Tan, L.W., Perozzi, G., Knight, D., Ruffin, R., Zalewski, P.: Anti-inflammatory effects of zinc and alterations in zinc transporter mRNA in mouse models of allergic inflammation. Am. J. Physiol. Lung Cell Mol. Physiol. **292**, 577–584 (2007). https://doi.org/10.1152/ajplung.00280.2006

Li, H., Li, M., Ran, X., Cui, J., Wei, F., Yi, G., Chen, W., Luo, X., Chen, Z.: The role of zinc in bone mesenchymal stem cell differentiation. Cell. Reprogram. **24**, 80–94 (2022). https://doi.org/10.1089/cell.2021.0137

Lin, Y.T., He, H., Kaya, H., Liu, H., Ngo, D., Smith, N.J., Banerjee, J., Borhan, A., Kim, S.H.: Photothermal atomic force microscopy coupled with infrared spectroscopy (AFM-IR) analysis of high extinction coefficient materials: a case study with silica and silicate glasses. Anal. Chem. **94**, 5231–5239 (2022). https://doi.org/10.1021/acs.analchem.1c04398

Liu, X., Rahaman, M.N., Day, D.E.: Conversion of melt-derived microfibrous borate (13–93B3) and silicate (45S5) bioactive glass in a simulated body fluid. J. Mater. Sci. Mater. Med. **24**, 583–595 (2013). https://doi.org/10.1007/s10856-012-4831-z

Mardas, N., Dereka, X., Stavropoulos, A., Patel, M., Donos, N.: The role of strontium ranelate and guided bone regeneration in osteoporotic and healthy conditions. J. Periodontal Res. **56**(2), 330–338 (2021). https://doi.org/10.1111/jre.12825

Oki, A., Parveen, B., Hossain, S., Adeniji, S., Donahue, H.: Preparation and in vitro bioactivity of zinc containing sol-gel-derived bioglass materials. J. Biomed. Mater. Res. Part A **69**, 216–221 (2004). https://doi.org/10.1002/jbm.a.20070

Pino, M., Stingelin, N., Tanner, K.E.: Nucleation and growth of apatite on NaOH-treated PEEK, HDPE and UHMWPE for artificial cornea materials. Acta Biomater. **4**, 1827–1836 (2008). https://doi.org/10.1016/J.ACTBIO.2008.05.004

Prasad, S., Datta, S., Adarsh, T., Diwan, P., Annapurna, K., Kundu, B., Biswas, K.: Effect of boron oxide addition on structural, thermal, in vitro bioactivity and antibacterial properties of bioactive glasses in the base S53P4 composition. J. Non Cryst. Solids. **498**, 204–215 (2018). https://doi.org/10.1016/j.jnoncrysol.2018.06.027

Ram, S., Ram, K.: IR and Raman studies and effect of γ radiation on crystallization of some lead borate glasses containing Al_2O_3. J. Mater. Sci. **23**, 4541–4546 (1988). https://doi.org/10.1007/BF00551957

Ram, S., Ram, K.: Infrared reflectance spectra and formalism of precipitation of acicular magnetic particles in network glasses. Infrared Phys. Technol. **37**, 457–469 (1996). https://doi.org/10.1016/1350-4495(95)00079-8

Rashad, M., Tekin, H.O., Zakaly, H.M., Pyshkina, M., Issa, S.A.M., Susoy, G.: Physical and nuclear shielding properties of newly synthesized magnesium oxide and zinc oxide nanoparticles. Nucl. Eng. Technol. **52**, 2078–2084 (2020). https://doi.org/10.1016/j.net.2020.02.013

Rau, J.V., Bonis, A.. De., Curcio, M., Schuhladen, K., Barbaro, K., Bellis, G.. De., Teghil, R., Boccaccini, A.R.: Borate and silicate bioactive glass coatings prepared by nanosecond pulsed laser deposition. Coatings **10**(11), 1105 (2020)

Saranti, A., Koutselas, I., Karakassides, M.A.: Bioactive glasses in the system $CaO–B_2O_3–P_2O_5$: Preparation, structural study and in vitro evaluation. J. Non Cryst. Solids **352**, 390–398 (2006). https://doi.org/10.1016/j.jnoncrysol.2006.01.042

Schuhladen, K., Wang, X., Hupa, L., Boccaccini, A.R.: Dissolution of borate and borosilicate bioactive glasses and the influence of ion (Zn, Cu) doping in different solutions. J. Non Cryst. Solids **502**, 22–34 (2018). https://doi.org/10.1016/j.jnoncrysol.2018.08.037

Schuhladen, K., Stich, L., Schmidt, J., Steinkasserer, A., Boccaccini, A.R., Zinser, E.: Cu, Zn doped borate bioactive glasses: antibacterial efficacy and dose-dependent: In vitro modulation of murine dendritic cells. Biomater. Sci. **8**, 2143–2155 (2020). https://doi.org/10.1039/c9bm01691k

Sengupta, S., Michalek, M., Liverani, L., Švančárek, P., Boccaccini, A.R., Galusek, D.: Preparation and characterization of sintered bioactive borate glass tape. Mater. Lett. **282**, 5–8 (2021). https://doi.org/10.1016/j.matlet.2020.128843

Subhashini, Bhattacharya, S., Shashikala, H.D., Udayashankar, N.K.: Synthesis and studies on microhardness of alkali zinc borate glasses. AIP Conf. Proc. **1591**, 749–750 (2014). https://doi.org/10.1063/1.4872742

Taha, T.A., Rammah, Y.S.: Optical characterization of new borate glass doped with titanium oxide. J. Mater. Sci. Mater. Electron. **27**, 1384–1390 (2016). https://doi.org/10.1007/s10854-015-3901-7

Thanasrisuebwong, P., Jones, J.R., Eiamboonsert, S., Ruangsawasdi, N., Jirajariyavej, B., Naruphontjirakul, P.: Zinc-containing sol-gel glass nanoparticles to deliver therapeutic ions. Nanomater. (Basel, Switzerland) **12**, 1691 (2022). https://doi.org/10.3390/nano12101691

Thyparambil, N.J., Gutgesell, L.C., Hurley, C.C., Flowers, L.E., Day, D.E., Semon, J.A.: Adult stem cell response to doped bioactive borate glass. J. Mater. Sci. Mater. Med. **31**, 1–8 (2020). https://doi.org/10.1007/s10856-019-6353-4

Wang, H., Zhao, S., Zhou, J., Shen, Y., Huang, W., Zhang, C., Rahaman, M.N., Wang, D.: Evaluation of borate bioactive glass scaffolds as a controlled delivery system for copper ions in stimulating osteogenesis and angiogenesis in bone healing. J. Mater. Chem. B **2**, 547–8557 (2014). https://doi.org/10.1039/C4TB01355G

Yamaguchi, M.: Role of nutritional zinc in the prevention of osteoporosis. Mol. Cell. Biochem. **338**, 241–254 (2010). https://doi.org/10.1007/s11010-009-0358-0

Yao, A., Wang, D., Huang, W., Fu, Q., Rahaman, M.N., Day, D.E.: In vitro bioactive characteristics of borate-based glasses with controllable degradation behavior. J. Am. Ceram. Soc. **90**, 303–306 (2007). https://doi.org/10.1111/j.1551-2916.2006.01358.x

Zhang, X., Jia, W.T., Gu, Y.F., Xiao, W., Liu, X., Wang, D.P., Zhang, C.Q., Huang, W.H., Rahaman, M.N., Day, D.E., Zhou, N.: Teicoplanin-loaded borate bioactive glass implants for treating chronic bone infection in a rabbit tibia osteomyelitis model. Biomaterials **31**, 5865–5874 (2010). https://doi.org/10.1016/j.biomaterials.2010.04.005

Zhao, S., Li, L., Wang, H., Zhang, Y., Cheng, X., Zhou, N., Rahaman, M.N., Liu, Z., Huang, W., Zhang, C.: Wound dressings composed of copper-doped borate bioactive glass microfibers stimulate angiogenesis and heal full-thickness skin defects in a rodent model. Biomaterials **53**, 379–391 (2015). https://doi.org/10.1016/j.biomaterials.2015.02.112

Authors and Affiliations

N. M. Salatein[1] · A. M. Abdelghany[2,3] · I. S. Fahim[1] · F. A. ElHussiny[4] · Y. Abdou[4]

✉ N. M. Salatein
namahmoud@nu.edu.eg

A. M. Abdelghany
a.m_abdelghany@yahoo.com

I. S. Fahim
isamy@nu.edu.eg

F. A. ElHussiny
Fathi_elhussiny@yahoo.com

Y. Abdou
yasser.abdou@science.tanta.edu.eg

[1] Smart Engineering Systems Research Center (SESC), Nile University, Cairo, Egypt

[2] Spectroscopy Department, Physics Research Institute, National Research Centre, 33 Elbehouth St, Dokki, Giza 12311, Egypt

[3] Department of Basic Science, Horus University, International Coastal Road, New Damietta, Damietta, Egypt

[4] Physics Department, Faculty of Science, Tanta University, Tanta, Egypt